

First order magnetic transition in CeFe₂ alloys: Phase-coexistence and metastability

S. B. Roy^{1,2}, G. K. Perkins¹, M. K. Chattopadhyay², A. K. Nigam³, K. J. S. Sokhey²,
P. Chaddah², A. D. Caplin¹ and L. F. Cohen¹

¹*Blackett Laboratory, Imperial College, London SW7 2BZ, UK*

²*Low Temperature Physics Laboratory, Centre for Advanced Technology, Indore 452013, India*

³*Tata Institute of Fundamental Research, Mumbai 400005, India*

(November 21, 2018)

Abstract

First order ferromagnetic (FM) to antiferromagnetic (AFM) phase transition in doped-CeFe₂ alloys is studied with micro-Hall probe technique. Clear visual evidence of magnetic phase-coexistence on micrometer scales and the evolution of this phase-coexistence as a function of temperature, magnetic field and time across the first order FM-AFM transition is presented. Such phase-coexistence and metastability arise as natural consequence of an intrinsic disorder-influenced first order transition. Generality of this phenomena involving other classes of materials is discussed.

75.30.Kz

The effect of quenched disorder on a first order phase transition has been a subject of considerable scientific interest since late 1970's¹. In condensed matter physics, several distinct examples are known; disordered- ferroelectric transitions², precursor effects in martensitic transitions³, the vortex matter phases of high temperature superconductors (HTS)⁴ and electronic phase-separation in manganites showing colossal magnetoresistance⁵. Of these the last two areas have drawn much attention in recent years, although without general recognition that there exists some common underlying physics. Detailed computational studies^{6,7} confirm the applicability of early theoretical picture¹ in manganites, and further emphasise that phase-coexistence can occur in any system in the presence of quenched disorder whenever two states are in competition through a first order phase transition. Here we choose to study a simple binary magnetic system CeFe₂ and show clear visual evidence of magnetic phase-coexistence on micrometer scales as the system is driven across the entire first order antiferromagnetic (AFM) to ferromagnetic (FM) transition. We explore how this phase-coexistence evolves as a function of temperature, magnetic field and time highlighting the generic features of a first order FM-AFM transition. The temporal evolution of the phase-coexistence demonstrates that nucleation and growth can lead to percolation of a particular phase and the existence of percolative behaviour is highly dependent on the random disorder landscape. This observation has important implications for other systems^{8,9} where percolative properties dominate macroscopic behaviour.

CeFe₂ is a cubic Laves phase ferromagnet (with Curie temperature ($\approx 230\text{K}$)¹⁰, where small substitution (<10 %) of selected elements such as Co, Al, Ru, Ir, Os and Re can induce a low temperature AFM state with higher resistivity than the FM state¹¹ . A giant magnetoresistance effect^{12,13} and various memory effects^{14,15} associated with the AFM-FM transition are well documented. We have chosen two CeFe₂ alloys with 4 and 5% Ru-doping for our present work. The preparation and characterisation of these polycrystalline alloys have been described in detail in ref. 11, and samples from the same batch have been well-characterised^{11,12,15–17}. Neutron diffraction studies of the same samples revealed a discontinuous change of the unit cell volume at the FM-AFM transition, confirming that it is

first order¹⁷. Bulk magnetic measurements were made with a vibrating sample magnetometer (Oxford Instruments) and a SQUID magnetometer (Quantum Design-MPMS5). The magnetic field profiles close to the sample surface were obtained using a scanning Hall probe system¹⁸ with 5 μm square InSb Hall sensors. The sensor was scanned at a distance of 7 μm from the sample surface, each image comprising of 256x256 pixels. Fields up to 40 kOe can be applied, and the stray induction from the sensor is so small (≈ 0.01 Oe) that it does not perturb the sample.

In fig. 1, the main panel shows the global magnetisation (M) versus temperature (T) in an applied field (H) of 5 kOe for the $\text{Ce}(\text{Fe}_{0.95}\text{Ru}_{0.05})_2$ sample (Ru-5). Two different measurement protocols were used: zero-field cooled (ZFC) and field-cooled cooling (FCC). The paramagnetic(PM)-FM transition is marked by the rapid rise of M with decreasing T below 200K and it is thermally reversible. The FM-AFM transition is marked by the sharp drop in M below 90K and shows substantial thermal hysteresis, which is an essential signature of a first order transition. We have obtained similar M - T curves for this sample as well as for the $\text{Ce}(\text{Fe}_{0.96}\text{Ru}_{0.04})_2$ sample (Ru-4) in various H . Thermal hysteresis is always present in the AFM-FM transition, and broadens with increasing H , so that when $H > 30$ kOe (15 kOe) for Ru-5 (Ru-4) the $M_{FCC}(T)$ and $M_{ZFC}(T)$ curves fail to merge at least down to 20K. Inset of Fig. 1 shows the schematic H-T phase diagram for the Ru-5 sample based on our $M(T)$ measurements with $T_{NW}(T_{NC})$ as the temperature of the sharp rise (fall) in M in the ZFC (FCC) path (see Fig. 1). T_{NC} is more closely defined as the temperature where dM/dT in the M vs T plot changes sign from negative to positive. T^* is the low temperature point where $M_{ZFC}(T)$ and $M_{FCC}(T)$ merges and T^{**} is the high temperature counterpart. A qualitatively similar phase diagram is obtained for the Ru-4 sample with lower characteristic temperatures. Note that $T_{NW}(H) < T_{NC}(H)$, i.e. the onset of nucleation of the AFM state on cooling occurs at a higher temperature than does nucleation of the FM phase during warming. This is an indication of a disorder-influenced first order transition. As discussed below, the sector of the (H,T) phase diagram shown in the inset to Fig. 1 bounded by the $T_{NC}(H)$ ($T_{NW}(H)$) and $T^*(H)$ ($T^{**}(H)$) lines is

metastable in nature and susceptible to energy fluctuations. We identify $T^*(H)$ ($T^{**}(H)$) as the low tempertaure (high temperature) limit of metastability in the free energy curves across a first order transition¹⁹. When the system is trapped in the metastable higher energy state it can be moved into the stable lower energy state by creating energy fluctuations such as cycling T or H- we refer to this process as "shattering" of the metastable state.

We shall address now on the issue of phase-coexistence and metastability in more details by exploring the FM-AFM transition region with isothermal field variation. In such isothermal experiments one is dealing with constant energy fluctautions (coming from $k_B T$ term) all along the transition region. In Fig.2 we present the global isothermal M-H curve of the Ru-5 sample at 60K. We also insert Hall-probe images taken at representative fields around this M-H curve, which are highly informative. In the ascending H-cycle there is a sharp rise in magnetization around 19 kOe indicating the onset of AFM-FM transition. In the H-regime below 19 kOe the sample is entirely in the AFM state, and the nature of the scanning Hall-probe field images remains same. Around 19 kOe random patches of high intensity local stray field appear in the sample, indicating the onset of FM phase in some parts of the sample. FM clusters of various size in the range of 5-20 micrometer are clearly distinguishable. The clusters grow in size and new clusters appear with further increase in H, and some of those merge to give rise to even larger clusters in the range 20-100 micrometer and this process continues until the whole sample reaches the FM state. While decrteasing field from 40 kOe, along with bulk magnetisation the Hall-images also show distinct thermal hysteresis. Traces of FM clusters remain down to 15 kOe, while the sample was completely in the AFM state in the regime $H < 19$ kOe in the ascending field path. We attribute this to supercooling of the FM state across the first order transition. We show here that a supercooled state i.e. 16 kOe in the descending H cycle, is susceptible to energy fluctuations. A small thermal perturbation in the form of an increase in temperature by 10 K and then bringing the sample back to 60K again, markedly decreases the amount of supercooled FM state. Note that the increase in T by 10 K should drive the system towards the higher temperature FM phase. However, the energy fluctuation associated with this temperature

cycling is detrimental for the supercooled FM state. We have seen very same features of phase-coexistence and metastability in micro-Hall probe scanning images, on temperature cycling across the AFM-FM transition while keeping the field constant. The detail results are not shown here for the sake of conciseness. Supercooling here is rationalised with the existence of a lower limit of metastability $T^*(H^*)$ in the free energy curve with the control parameter $T(H)$ ¹⁹. We might expect to see a signature of superheating in the same way. The trace of superheated AFM state would remain as a shaded region in an almost completely illuminated image frame. Better resolution of the images is required to reach a firm conclusion in this regard, and locate an upper limit of metastability temperature (field) $T^{**}(H^{**})$.

The sample used for Hall-imaging here is of dimension 2mmx1.2mmx1.2mm, and the images are obtained by zooming on an area of 1mm x 1mm in the central portion of the sample away from the edges. The whole set of experiments were repeated for another sample of dimension 1mmx1.2mmx1.2mm. Exactly the same features are observed, which negates any dominant role of sample geometry. The Hall-probe images taken across the FM-PM transition of both the samples show a continuous decrease of uniformly distributed field intensity, which is both consistent with a second order phase transition and confirmation that the samples are macroscopically chemically homogeneous. We can further rule out gross chemical phase separation with the results of X-ray diffraction¹¹ and neutron scattering¹⁷ studies. We assert here that purely statistical quenched compositional disorder is at the root of the phase-coexistence observed here. Precisely this kind of intrinsic compositional disorder is thought to give rise to "tweed structure" in the vicinity of martensitic transitions³ and to phase-separation on sub-micrometer scale in manganites⁵⁻⁷. The influence of intrinsic compositional disorder (through Ru-substitutions) on the critical fluctuations phenomena at the second order PM-FM transition in the present CeFe₂ alloys has earlier been studied through detailed magnetic measurements¹⁶.

The regions in the Ru-5 sample which go to the FM state first in the ascending field cycle (Fig.2) are very different from those which transform first to the AFM state in the

descending field cycle (Fig.2). This is indicative of the local variation of the AFM-FM transition temperature T_N or field H_M leading to a rough $T_N(x,y)$ or $H_M(x,y)$ landscape. This distribution of T_N and H_M gives rise to the impression of global rounding of the transition in the bulk measurements. Our observation is in consonance with the disordered influenced first order transition proposed by Imry and Wortis¹. A very similar disorder induced rough landscape picture has earlier been proposed for the vortex solid melting in the HTS material BSCCO⁴ and materials with a pre-martensitic transition³. We have already seen that the traces of the supercooled-FM phase remain in fields well below the onset temperature field of the FM state in the ascending field cycle. If there was a single first order transition field H_M (temperature T_N) the FM clusters would have appeared in the ascending field cycle in the sample first at the positions with relatively low energy barrier for the nucleation of the stable FM phase . Using the same argument, in the descending field cycle the stable AFM phase would appear first at these very points, and these spots should have been the spots of lower field intensity. However, the first FM-patches not only survived in the descending field cycle, but some actually continued to exist as supercooled metastable FM state (see Fig.2). The very same features are observed in the temperature variation measurements (not shown here). This again emphasised a rough $T_N(x,y)$ - $H_M(x,y)$ landscape picture.

We provide additional evidence that the phase-coexistence regime bounded by $T_{NC}(H)$ ($T_{NW}(H)$) and $T^*(H)$ ($T^{**}(H)$) line (see inset of Fig.1) indeed metastable. Fig. 3 shows snap shots of the temporal evolution of the FM-phase clusters while undergoing the field induced AFM-FM transition. In these images T is fixed at 60K and H is fixed at 20 kOe after starting from zero field in the ZFC condition. Twenty scanning Hall-probe images are taken over a period of 168 minutes and two representative images have been selected. Significant temporal growth of the FM clusters after their initial nucleation at random positions of the sample is clearly visible. This is also a strong indication that the AFM state is superheated at least in some regions of the sample.

We have observed qualitatively similar features of phase-coexistence and metastability

in the Ru-4 sample both in the bulk magnetization and Hall-imaging studies. In this sample with less doping the growth of the FM phase at the onset of the AFM-FM transition, both as a function of T and H, is faster than the Ru-5 sample. Growth rate can be correlated directly with the sharpness of the M-T and M-H curves in this sample¹⁵. This relatively fast growth process along with the smaller number of nucleating clusters prohibited a clear-cut observation of the cluster size distributions in the phase-coexistence regime in the imaging experiments. Moreover it is now demonstrated here the way different disorder landscapes can control nucleation and growth. The key point is that if growth is slow enough, percolation will occur over an observable H (or T) interval before phase coexistence collapses. In the present study this is clearly true for the $x = 0.5$ sample. Percolative behaviors can be controlled by quite subtle changes in sample doping. The ramification to the manganite system , for example, is obvious.

In conclusion then we have imaged FM-AFM phase-coexistence across the AFM-FM transition in two $\text{Ce}(\text{Fe},\text{Ru})_2$ alloys. This AFM-FM transition bears distinct signatures of a first order phase transition namely, supercooling, superheating and time-relaxation. We have imaged the temporal growth of the clusters inside the phase co-existence regime for the first time and shown that this regime is quite sensitive to any energy fluctuations. Phase-coexistence and metastability arise as a consequence of the intrinsic disorder influenced first order transition⁵⁻⁷. The clusters in the present phase-coexistence regime have a size distribution in the range of 5-100 micrometer. This is larger than the length scale of $0.5 \mu\text{m}$ observed previously in manganites^{5,8} and discussed in the existing theories⁵⁻⁷. The smallest size of clusters which can be detected in our present study is limited by the resolution of the Hall-probe ($5 \mu\text{m}$). However, the growth and merger of the clusters as a function of T, H and time lead naturally to the observation of a range of cluster size. It will be interesting now to see whether such a wide scale of cluster size distribution extending to micrometer scales is possible within the existing class of theoretical models^{6,7} or whether our observations stimulate further theoretical refinement. Comparing further with the rough landscape picture of the vortex-matter melting transition⁴, our observation highlights the

generality of the phase-coexistence phenomenon. This in turn points to the possibility of the key role of intrinsic disorder influenced first order transitions in other classes of material of current interest namely giant magneto-caloric materials^{21,22} and magnetic shape memory alloys²³.

SBR acknowledges financial support in the form of a EPSRC visiting fellowship.

REFERENCES

- ¹ Y. Imry and M. Wortis, Phys. Rev. **B19**, 3580 (1979).
- ² H. Scjhremmer, W. Kleemann and D. Rytz, Phys. Rev. Lett. **62**, 1896(1989).
- ³ S. Kartha, J. A. Krumhansl, J. P. Sethna and L. K. Wickham, Phys. Rev. **B52**, 803 (1995).
- ⁴ A Soibel et al, Nature(London) **406** 283 (2000).
- ⁵ E. Dagotto, T. Hotta and A. Moreo, Phys. Rep. **344** 1 (2001) ; E. Dagotto, The Physics of Manganites and Related Compounds (Springer, 2003) (and references there in).
- ⁶ A. Moreo et al, Phys. Rev. Lett. **84**, 5568 (2000).
- ⁷ J. Burgy et al, Phys. Rev. Lett. **87** 277202 (2001).
- ⁸ M. Uehara, S. Mori, C. H. Chen and S. W. Cheong, Nature **399** 560 (1999).
- ⁹ L. Zhang et al, Science **298** 805 (2002).
- ¹⁰ L. Paolisini et al, Phys. Rev. **B58** 12117 (1998) (and references therein).
- ¹¹ S. B. Roy and B. R. Coles, J. Phys.:Condens. Matter **1** 419 (1989); Phys. Rev. **B39** 9360 (1990).
- ¹² H. Kunkel et al, Phys. Rev.**B53** 15099 (1996).
- ¹³ H. Fukuda et al Phys. Rev. **B63** 054405 (2001).
- ¹⁴ M. A. Manekar et al, Phys. Rev. **B64** 104416 (2001).
- ¹⁵ M. K. Chattopadhyay et al. Phys. Rev. **B68** 174404(2003); K. J. S. Sokhey et al, Solid St. Commun. **129** 19 (2003).
- ¹⁶ D. Wang, H. P. Kunkel and G. Williams, Phys. Rev. **B51** 2872 (1995).
- ¹⁷ S. J. Kennedy and B. R. Coles, J. Phys.:Condens. Matter **2** 1213 (1990).

¹⁸ G. K. Perkins et al Supercond. Sci. Tech. **15** 1156 (2002).

¹⁹ P. M. Chaikin and T. C. Lubensky, Principles of Condensed Matter Physics (Cambridge University Press, Cambridge, England, 1995); P. Chaddah and S. B. Roy, Phys. Rev. **B60** 11926 (1999).

²⁰ Taking the intensity of the FM state as a reference, the AFM state is represented by field intensity less than 20% of this value (black) while white regions represent intensities greater than 20% of this value. At the onset of the FM transition the FM-clusters of higher field intensity appear at random position across the sample and they vary in size. The whole process of this AFM-FM transition both in the ascending and descending field cycle can be seen in a movie available at the web-site...

²¹ B. Teng et al, J. Phys.: Condens. Matter. **14** 6501 (2002).

²² V. Pecharsky et al. Phys. Rev. Lett. **91** 197204 (2003).

²³ W-H Wang et al. Phys. Rev. **B65** 012416 (2001).

FIGURES

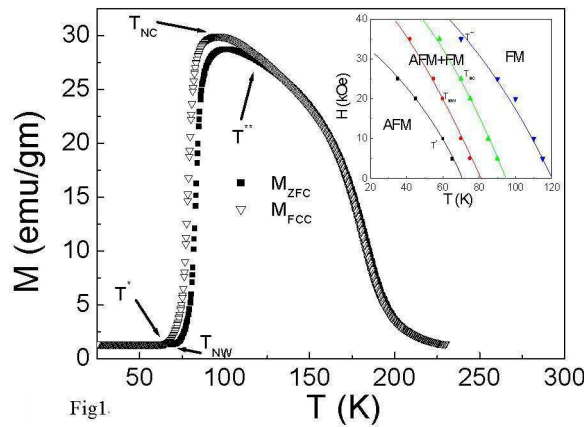


FIG. 1. M versus T in an applied H of 5 kOe for the Ru-5 sample, in ZFC and FCC mode. Inset shows the H - T phase diagram representing T_{NW} , T_{NC} , T^* and T^{**} (see text for their definitions) as a function of H . The value of T^* goes below 20K when $H > 30$ kOe.

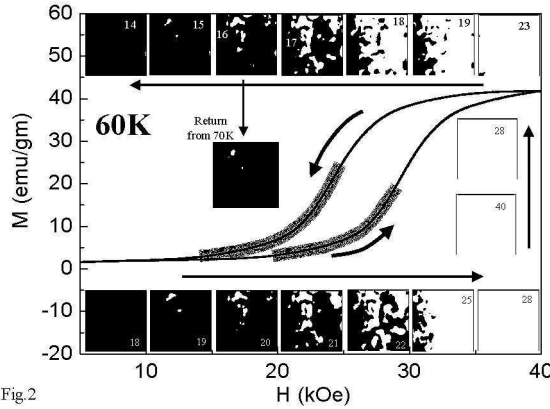


FIG. 2. Isothermal M versus H plot at 60K after cooling in zero magnetic field. The representative Hall probe images are inserted around the main figure. Starting counter-clockwise from the bottom left hand corner the images represent the AFM state in the ascending field cycle ($H=18$ kOe), AFM-FM transition regime in the ascending field cycle ($H=19, 20, 21, 22, 25, 28$ kOe) , FM state ($H=40$ kOe), FM-AFM transition regime in the descending field cycle ($H=28, 23, 19, 18, 17, 16, 15$ kOe) and the final AFM state ($H=14$ kOe) at the end of the cycle . Each frame covers an area of 1×1 mm in the central portion of a sample of dimension 2 mm \times 1.2 mm \times 1.2 mm. The field intensity distribution in the images is uniform in the FM state and AFM state with the intensity of the AFM state being much less than the FM state. We choose a 20% criterion²⁰ to highlight the onset of the AFM-FM transition in the region marked by the black band. It, however, may give the wrong impression that the formation of FM state is completed by 26 kOe. The FM state actually goes on developing on the ascending field path until 35 kOe, and these developments in the higher T regime can be visualised on choosing a higher ($>20\%$) threshold criterion The frame below 16 kOe in the top row shows the effect of temperature cycling of 10 K on the supercooled FM state at 16 kOe.

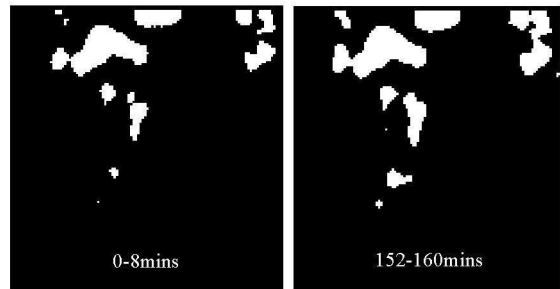


Fig. 3

FIG. 3. Images showing temporal evolution of the phase-coexistence at 20 kOe during the isothermal field induced AFM-FM transition at 60K. Two images were taken 160 minutes apart, with each image taking 8 minutes of experimental time to complete. The sample area scanned and the criterion for the colour code of the image remain same as in Fig.2.